Interaction of a skewed Rankine vortex pair

S. Jayavel,[a] Pratish P. Patil,[b] and Shaligram Tiwari[c]
Department of Mechanical Engineering, Indian Institute of Technology Madras, Chennai 600036, India

(Received 16 November 2007; accepted 20 July 2008; published online 13 August 2008)

An analytical investigation is carried out to study the kinematics of a fluid particle in an interacting field of a skewed pair of fixed Rankine vortices. A general formulation governing the kinematics of a fluid particle has been presented based on the superposition of the velocity field due to each vortex in the pair. The kinematics of a Lagrangian fluid particle is found to be governed by a nonlinear dynamical system. The fixed or stationary points of the dynamical system have been identified analytically and their existence is confirmed by the nature of particle paths in the neighborhood of fixed points. The nature of the particle path and velocity signal is reported for general as well as special configurations of the vortex pair in the presence and absence of an external uniform flow. As a specific application of the proposed problem, superimposition of the translational velocity on a semi-infinite field of longitudinal vortices generated by vortex generators mounted on fin plates of heat exchangers has also been studied. © *2008 American Institute of Physics*.
[DOI: 10.1063/1.2969115]

I. INTRODUCTION

Laminar flows under certain conditions can produce chaotic particle paths, leading to enhanced transport and mixing characteristics. Vortex generators mounted on fins in fin-tube and fin-plate heat exchangers enhance heat transfer by promoting flow mixing and improving fluid transport. It is primarily because the longitudinal or streamwise vortices generated by vortex generators destabilize the growth of the hydrodynamic boundary layer and disrupt the growth of the thermal boundary layer.[1] In the case of fin-tube heat exchangers, the streamwise vortices also reduce the size of the dull wake zone behind the tubes. It is of interest to researchers to investigate the underlying mechanism responsible for the vortex enhancement in heat transfer. In general, the vortex system may be either fixed or moving. For example, the streamwise vortices generated by fixed vortex generators mounted on fins of heat exchangers form a system of fixed vortex filaments. If the vortices of a given physical system are not fixed, the consequences may lead to vortex merging. Romero-Mendez *et al.*[2] studied the influence of Rankine vortices in an inviscid thermal boundary layer flow for different vortex orientations. Moffatt[3] studied the interaction of two propagating vortex pairs, each pair being aligned along the principal axis of strain associated with the other that is skewed in space.

The existence of chaotic path lines in a flow field is predicted using the Lagrangian approach of tracking an individual fluid particle. Casciola and Piva[4] employed the Lagrangian approach to investigate vorticity intensification in swirling rings. The dynamics of a single vortex tube in an inviscid fluid is reduced to a simple form, which indicates that for very small core sizes, the motion of vortex tube follows the dynamics given by the Biot–Savart equations, as suggested by Moore and Saffman.[5] For a comprehensive discussion on vorticity dynamics, one may refer to Ref. 6. The equations governing fixed vortices do not remain valid for the case of interacting vortex pairs with a small axial separation due to core merging and thereby core deformation taking place. Meunier *et al.*[7] proposed a quantitative criterion for merging of a pair of equal two-dimensional corotating vortices for the case of two approaching vortex filaments by computing nonlinear Euler solutions. Le Dizes and Verga[8] studied the viscous interaction of two corotating vortices before merging using direct numerical simulations of Navier–Stokes equations. Siggia[9] showed that the evolution of a single vortex filament through merging leads to a pairing effect and then to a violent stretching that ends up in shrinkage of the core to zero size in a finite time.

The kinematic analysis of motion of a Lagrangian fluid particle in the field of interacting vortices aims at possible chaotic motion of fluid particles. In general, the equations governing the kinematics of a fluid particle in an interacting vortex field form a nonlinear dynamical system. A detailed study of the dynamical system approach towards kinematics of mixing has been presented by Ottino.[10] The basic criterion for the resulting nonlinear dynamical system to become chaotic is its nonintegrability. For the case of two point vortices in a plane with a constant distance between their axes, the integrability has been confirmed by Batchelor.[11] Aref and Pomphrey[12] showed that the system of three point vortices in a plane is also integrable, and the system of four or more vortices in an unbounded two-dimensional region is, in general, chaotic. The study of flow mixing requires trajectory analysis of moving fluid elements over extended times. The points over one pseudoperiod, where no net motion appears, may be treated as fixed points. In a flow field, identifying the existence of a fixed point and analysis of the nature of stability of the system in the neighborhood of such a point are of fundamental interest. This is primarily because in the neighborhood of fixed points, the transport characteristics of

[a]Electronic mail: me06d015@smail.iitm.ac.in.
[b]Electronic mail: pratish@smail.iitm.ac.in.
[c]Electronic mail: shaligt@iitm.ac.in.

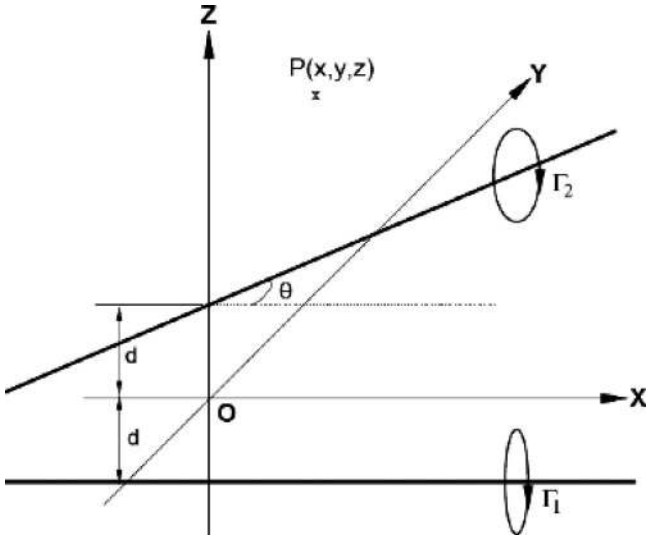

FIG. 1. Configuration of two skewed and inclined Rankine vortices with a viscous core.

the flow are poor and in many situations their existence is undesirable.

In the present work, an interacting vortex field has been considered in which the kinematics of a Lagrangian fluid particle due to the combined influence of two fixed Rankine vortex filaments has been investigated. The system of equations governing the kinematics of the fluid particle gives rise to a nonlinear dynamical system. For such a dynamical system, the phase space mimics the physical space identically. For carrying out stability analysis of the dynamical system, it is essential to identify the stationary points or fixed points of the system. The existence of fixed points of the present dynamical system has been investigated analytically for general and particular configurations of the considered vortex pair. As a special case of the considered vortex pair configuration, the case of an interacting parallel vortex pair mimics the situation arising in interaction of streamwise vortices generated by vortex generators mounted on fins of heat exchangers,[1] Moreover, the vortex systems considered by Vasudevan *et al.*[13] for the case of fin-plate heat exchangers and Tiwari *et al.*[14] for fin-tube heat exchangers are special cases of the parallel vortex pair generating a semi-infinite velocity field with a superimposed uniform flow. The present study also reports the effect of an external uniform flow on the nature of the path and velocity signal of a fluid particle in the field of the fixed Rankine vortex pair for its general as well as special configurations.

II. GOVERNING KINEMATIC EQUATIONS

A. Velocity field of a single Rankine vortex

Figure 1 shows a system of two fixed vortex filaments which have their axes inclined at an angle θ and skewed in space with a separation distance of $2d$. Each of the vortices is a Rankine vortex which is free and inviscid in nature and has a viscous core of radius a. The velocity of a fluid particle located within the vortex core has rigid body rotation and outside the core, the velocity field is governed by that of a free inviscid vortex. The flow field resulting due to such a Rankine vortex system corresponds to potential flow solutions of Euler equations. In the case of potential flow situations, we know that the velocity fields can be obtained by the superimposed field of various potential flow contributors. For a single vortex, the velocity vector of the fluid particle is given as

$$\vec{V} = \frac{\Gamma}{2\pi a^2} r \hat{e}_\phi \quad \text{for } r \le a, \tag{1a}$$

$$\vec{V} = \frac{\Gamma}{2\pi r} \hat{e}_\phi \quad \text{for } r > a, \tag{1b}$$

where Γ is the vortex strength, a is the core radius, and $\hat{e}_\phi$ is the tangential unit vector at any general point on the circle of radius r.

B. Velocity field of a skewed pair of Rankine vortices

In Fig. 1, if the circulation strength of the two vortices are assumed to be Γ_1 and Γ_2, the velocity vector of a representative Lagrangian fluid particle in the combined field of both the vortices is given as

$$\vec{V}_P \equiv \frac{dx}{dt}\hat{i} + \frac{dy}{dt}\hat{j} + \frac{dz}{dt}\hat{k},$$

$$\vec{V}_P \equiv \vec{V}_1 + \vec{V}_2,$$

where $\vec{V}_1$ is the velocity vector due to the first vortex and $\vec{V}_2$ is the velocity vector due to the second vortex. Thus

$$\vec{V}_P = \frac{\Gamma_1}{2\pi a^2} r_1 \hat{e}_{\phi_1} + \frac{\Gamma_2}{2\pi r_2} \hat{e}_{\phi_2} \quad \text{for } r_1 < a \quad \text{and } r_2 > a, \tag{2a}$$

$$\vec{V}_P = \frac{\Gamma_1}{2\pi r_1} \hat{e}_{\phi_1} + \frac{\Gamma_2}{2\pi a^2} r_2 \hat{e}_{\phi_2} \quad \text{for } r_1 > a \quad \text{and } r_2 < a, \tag{2b}$$

$$\vec{V}_P = \frac{\Gamma_1}{2\pi r_1} \hat{e}_{\phi_1} + \frac{\Gamma_2}{2\pi r_2} \hat{e}_{\phi_2} \quad \text{for } r_1 > a \quad \text{and } r_2 > a. \tag{2c}$$

Here, $\hat{e}_{\phi_1}$ and $\hat{e}_{\phi_2}$ are the tangential unit vectors to the circular paths around the first and second vortices, respectively; r_1 and r_2 are the perpendicular distances of the fluid particle from the axes of the two vortices. Using the coordinate system shown in Fig. 1 in which the origin of the coordinates is located at the midpoint of the shortest separation line between the axes of the two vortices, expressions for r_1 and r_2 can be written as

$$r_1 = [y^2 + (z+d)^2]^{1/2}, \tag{3a}$$

$$r_2 = [y'^2 + (z-d)^2]^{1/2}, \tag{3b}$$

where the transformed coordinates and their respective unit vectors are related to the original coordinates as

$$x' = x\cos\theta + y\sin\theta, \quad \hat{i}' = \cos\theta\hat{i} + \sin\theta\hat{j}, \tag{4a}$$

$$y' = -x\sin\theta + y\cos\theta, \quad \hat{j}' = -\sin\theta\hat{i} + \cos\theta\hat{j}. \tag{4b}$$

The unit vectors $\hat{e}_{\phi_1}$ and $\hat{e}_{\phi_2}$ are given as

$$\hat{e}_{\phi_1} = -\sin\phi_1\hat{j} + \cos\phi_1\hat{k}, \quad \hat{e}_{\phi_1} = -\frac{z+d}{r_1}\hat{j} + \frac{y}{r_1}\hat{k}, \tag{5a}$$

$$\hat{e}_{\phi_2} = -\sin\phi_2\hat{j}' + \cos\phi_2\hat{k}, \quad \hat{e}_{\phi_2} = -\frac{z-d}{r_2}\hat{j}' + \frac{y'}{r_2}\hat{k}. \tag{5b}$$

C. Nonlinear dynamical system

Substituting Eqs. (3)–(5) into Eq. (2), we obtain the dynamical system governing the kinematics of a Lagrangian fluid particle located at a point $P(x,y,z)$. The dynamical system can be nondimensionalized with respect to the length scale of a (core radius) and the time scale of $\tau=\Gamma/2\pi a^2$, where $\Gamma_1=\alpha\,\Gamma$ and $\Gamma_2=\beta\,\Gamma$. The half-separation between the axes of the two vortices is nondimensionalized as $\varepsilon=d/a$. For simplicity of presentation, the symbols of variables are retained unchanged after nondimensionalization. The resulting dimensionless form of the nonlinear dynamical system becomes

$$\frac{dx}{dt} = \frac{\beta(z-\varepsilon)\sin\theta}{A_2}, \tag{6a}$$

$$\frac{dy}{dt} = \frac{-\alpha(z+\varepsilon)}{A_1} - \frac{\beta(z-\varepsilon)\cos\theta}{A_2}, \tag{6b}$$

$$\frac{dz}{dt} = \frac{\alpha y}{A_1} + \frac{\beta(y\cos\theta - x\sin\theta)}{A_2}, \tag{6c}$$

where A_1 and A_2 are functions of the inclination angle between the two vortices, their axial separation, and position of the fluid particle. During the motion of the fluid particle and its relative position with respect to the two vortices, A_1 and A_2 take the functional form as

$$A_1 = 1, \quad A_2 = (y\cos\theta - x\sin\theta)^2 + (z-\varepsilon)^2 \quad (\text{for } r_1 < 1 \text{ and } r_2 > 1), \tag{7a}$$

$$A_1 = y^2 + (z+\varepsilon)^2, \quad A_2 = 1 \quad (\text{for } r_1 > 1 \text{ and } r_2 < 1), \tag{7b}$$

$$A_1 = y^2 + (z+\varepsilon)^2, \quad A_2 = (y\cos\theta - x\sin\theta)^2 + (z-\varepsilon)^2 \quad (\text{for } r_1 > 1 \text{ and } r_2 > 1). \tag{7c}$$

The nondimensionalized systems of nonlinear ordinary differential equations are solved numerically to obtain the time dependence of the position and transverse components of the velocities of the fluid particle.

III. FIXED POINTS

The fixed points or stationary points of a dynamical system correspond to the stationary solutions of the system of equations constituting the dynamical system. The neighborhood of stationary points in a fluid medium possesses poor transport properties. In vortex dominated flows, the fixed or stationary points are the locations near which the fluid is almost stagnant. If the fixed point becomes a center, the trajectories of fluid particles around it form periodic closed orbits. Hence, the identification of fixed points becomes important in the perspective of advection transport of fluid particles. In the situations where the objective is to enhance fluid mixing by chaotic advection,[15] the existence of fixed points is undesired and identification of flow regions with poor transport properties becomes an essential part of the study. The nature of a fixed point depends on the eigenvalues of the linearized form of the respective dynamical system in the vicinity of the fixed point.[16] The fixed points of the present dynamical system are obtained by simultaneous solution of equations resulting after equating the right-hand-side terms to zero in the set of equations (6a)–(6c), i.e., $dx/dt=0$, $dy/dt=0$, and $dz/dt=0$.

A. Fixed points of the parallel vortex pair

For the system of skewed ($\varepsilon\neq 0$) and parallel vortices ($\theta=0$) with equal strength ($|\alpha|=|\beta|=1.0$), the general dynamical system reduces to

$$\frac{dx}{dt} = 0, \tag{8a}$$

$$\frac{dy}{dt} = -\frac{\alpha(z+\varepsilon)}{A_1} - \frac{\beta(z-\varepsilon)}{A_2}, \tag{8b}$$

$$\frac{dz}{dt} = \frac{\alpha y}{A_1} + \frac{\beta y}{A_2}. \tag{8c}$$

Here the signs of the terms on the right hand side depend on relative algebraic values of α and β. Moreover, for $\theta=0$, the functions A_1 and A_2, depending on the relative position of the fluid particle, reduce to the form

$$A_1 = 1, \quad A_2 = y^2 + (z-\varepsilon)^2 \quad (\text{for } r_1 < 1 \text{ and } r_2 > 1),$$

$$A_1 = y^2 + (z+\varepsilon)^2, \quad A_2 = 1 \quad (\text{for } r_1 > 1 \text{ and } r_2 < 1),$$

$$A_1 = y^2 + (z+\varepsilon)^2, \quad A_2 = y^2 + (z-\varepsilon)^2 \quad (\text{for } r_1 > 1 \text{ and } r_2 > 1).$$

The values of α and β depend on the sense of rotation of the vortices in the pair. Figures 2(a)–2(d) show four different combinations of parallel vortex pairs generated by winglet-type vortex generators mounted on fin plates, viz., $\alpha=1$, $\beta=-1.0$; $\alpha=\beta=1.0$; $\alpha=-1$, $\beta=1.0$, and $\alpha=\beta=-1.0$, respectively.

In the case of the *corotating* configuration of the vortex pair, i.e., $\alpha=\beta=1.0$, it is apparent from Eqs. (8a)–(8c) that $x=y=z=0$ is a fixed point resulting as a trivial solution of the dynamical system. However, no real fixed points are found to

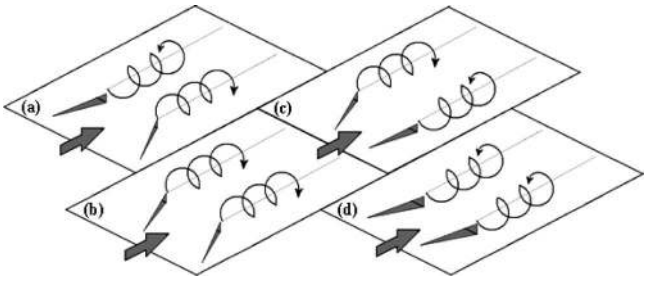

FIG. 2. Longitudinal fixed vortex filaments generated by winglet-type vortex generators mounted on a fin plate: (a) $\alpha=1$, $\beta=-1$, (b) $\alpha=1$, $\beta=1$, (c) $\alpha=-1$, $\beta=1$, and (d) $\alpha=-1$, $\beta=-1$.

exist for $y\neq 0$. On the other hand, for $y=0$, there exist two fixed points in the y-z plane for all values of x, viz., $z=\sqrt{\varepsilon^2-1}$ and $z=-\sqrt{\varepsilon^2-1}$. Thus, for $\varepsilon=2$, the locus of fixed points is identified as $y=0$, $z=\pm\sqrt{3}$ $\forall x$. In a similar way, for the *counter-rotating* configuration of the vortex pair, i.e., $\alpha=1.0$ and $\beta=-1.0$, the real fixed points are found to exist only for $y=0$, being given as $z=\pm\sqrt{\varepsilon^2+1}$. Consequently, the locus of the fixed points becomes $y=0$, $z=\pm\sqrt{5}$ $\forall x$.

B. Fixed points of the oblique and skewed vortex pair

For oblique and skewed likewise vortex pair, i.e., $\varepsilon\neq 0$, $\theta\neq 0$, to obtain the stationary points, we equate the right-hand-side terms in the set of equations (6a)–(6c) to zero,

$$\frac{dx}{dt}=\frac{\beta(z-\varepsilon)\sin\theta}{A_2}=0\Rightarrow z=\varepsilon.$$

Consequently, substituting $z=\varepsilon$ in Eq. (6b) and equating to zero reduces to

$$\frac{dy}{dt}=\frac{-\alpha(2\varepsilon)}{A_1}=0\Rightarrow\varepsilon=0.$$

However, the present formulation pertaining to a skewed vortex pair does not entertain the case of a coplanar and intersecting vortex pair. This is due to its vortex core interactions and possible core deformations which eliminate any possibility of $\varepsilon=0$ and is an infeasible solution independent of functions A_1 and A_2. This deduces the fact that all the velocity components cannot vanish simultaneously and thus no real fixed points are expected to exist.

An obvious interesting question that arises is what happens to the points that are already identified as stationary points for a parallel vortex pair system when the vortex pair becomes oblique by a small angle. The computations are carried out for these cases corresponding to $\varepsilon=2$ with a starting point as $y=0, z=\pm\sqrt{3}$ $\forall x\in R$, which is a fixed point for a parallel vortex pair system as shown in Sec. III A. The observation is focused on the evolving velocity phase plots. The phase plots for different angles between the vortices of the pair, viz., $\theta=0°$, 5°, 15°, 30°, 60°, and 90° are presented in Figs. 3(a)–3(f). For parallel vortex pairs, i.e., $\theta=0°$, the starting point is a stationary one and so all the velocity components, viz., u, v, and w, equal to zero at all instants of time; thereby the velocity phase plot is simply a point with u, v, and $w=0$, as shown in Fig. 3(a). As the inclusion angle between the oblique vortices increases, the velocity phase plots show a growing spread, as can be seen in Figs. 3(b)–3(f). This indicates that the stationary fixed points do not exist in the field of an oblique likewise vortex pair.

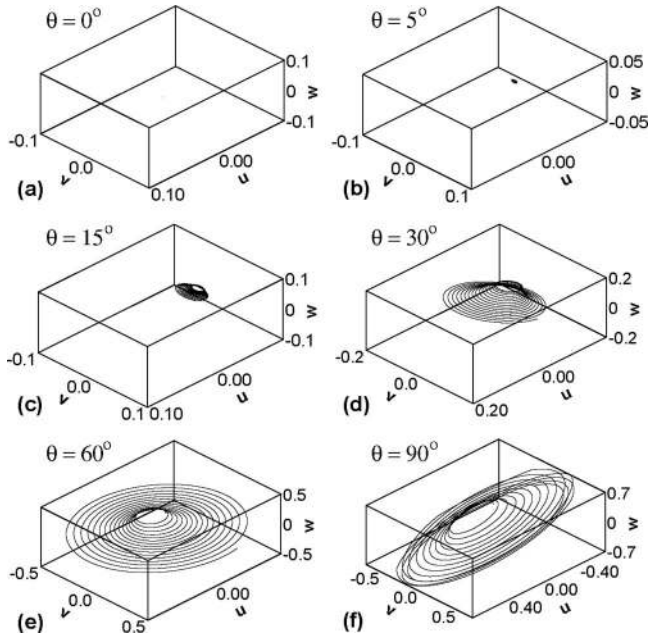

FIG. 3. Velocity phase plots of a Lagrangian fluid particle initially located at $y=0$, $z=\sqrt{3}$, $\forall x\in R$ for different angular orientations of the oblique vortex pair.

It is observed that the dynamical system in its presented general form, as represented by Eqs. (6a)–(6c), has no real fixed points for $\varepsilon\neq 0$, and $\theta\neq 0$. Consequently, the field of the oblique and skewed vortex pair is expected to be free of localized dull zones responsible for poor transport of momentum, energy, and concentration.

IV. RESULTS AND DISCUSSION

A. Inclined and skewed vortex pair

Figures 4(a)–4(d) present the paths of a fluid particle for four different angular orientations of $\theta=0°$, 30°, 60°, and 90° for the Rankine vortex pair corresponding to $\alpha=1$, $\beta=-1.0$. The axial half-separation of the skewed pair is fixed and equal to $\varepsilon=2.0$. For all the paths corresponding to different values of θ, the initial position of the fluid particle is chosen as the center of the upper vortex ($x_0=0.0$, $y_0=0.0$, and $z_0=2.0$) and the nondimensional time for the motion of the particle is $t=100$. In Fig. 4(a), for $\theta=0°$, the path of the fluid particle remains confined in a plane normal to the x axis and the particle is virtually constrained to revolve around the axis of the upper vortex. For larger values of θ, the path becomes three dimensional and shows wider zones of spreading. In Figs. 4(b)–4(d), the particle initially being at the center of the upper vortex has a little influence due to the field of the lower vortex. Figures 5(a) and 5(b) present transverse velocity signals, v and w, respectively, of the fluid particle corresponding to the four different paths shown in Figs. 4(a)–4(d). Since the fluid particle starts from a location

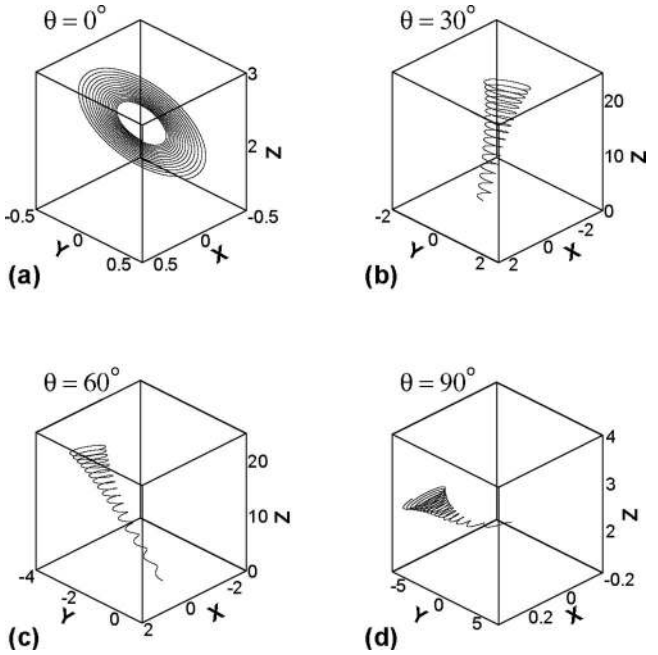

FIG. 4. Path of a fluid particle for four different angular orientations of the skewed Rankine vortex pair (α=1.0, β=−1.0, ε=2.0; x_0=0.0, y_0 =0.0, z_0=2.0; t=100).

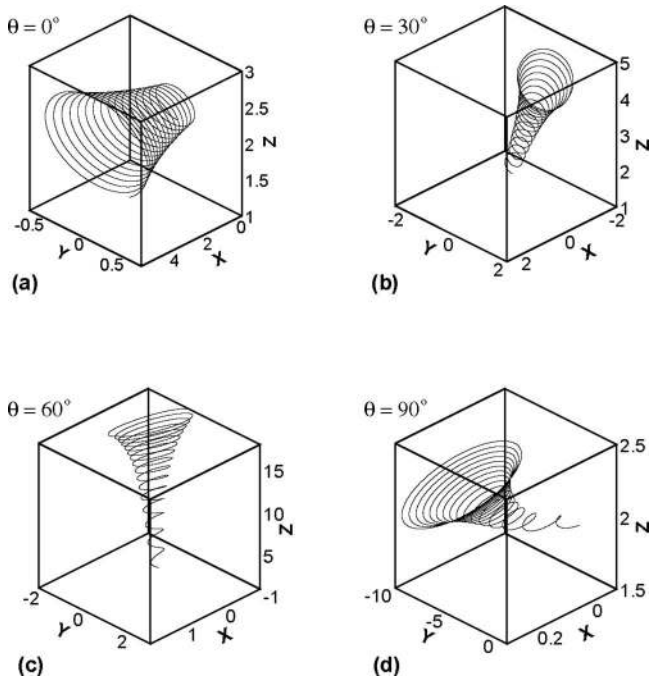

FIG. 6. Path of a fluid particle for four different angular orientations of the skewed Rankine vortices (α=1.0, β=−1.0, ε=2.0; x_0=0.0, y_0=0.0, z_0=2.0; t=100) with a superimposed uniform velocity in the x direction (u_0=0.05).

on the axis of one of the vortex, as it moves away from the axis, its velocity keeps increasing until it reaches the core radius of the respective vortex, which is apparent from Figs. 5(a) and 5(b). As the angle between the two vortices increases, the amplitude of transverse velocity decreases. This is basically due to the diminishing magnitude of the transverse velocity components for larger angles.

B. Superposition of external flow on the inclined vortex system

Figures 6(a)–6(d) present the paths of a fluid particle for similar angular orientations and initial positions as presented in Figs. 4(a)–4(d), corresponding to α=1, β=−1.0. The velocity field due to the Rankine vortex pair is superimposed with a uniform flow in the x direction to mimic the practical situation. The axial half-separation of the skewed pair is fixed and equal to ε=2.0. A comparison of Figs. 4(a) and 6(a) shows the effect of the superimposed uniform external flow on the path of the fluid particle where in the latter case, the resulting helical path is due to uniform transport. Figures 7(a) and 7(b) present transverse velocity signals, v and w, respectively corresponding to four different paths shown in Figs. 6(a)–6(d).

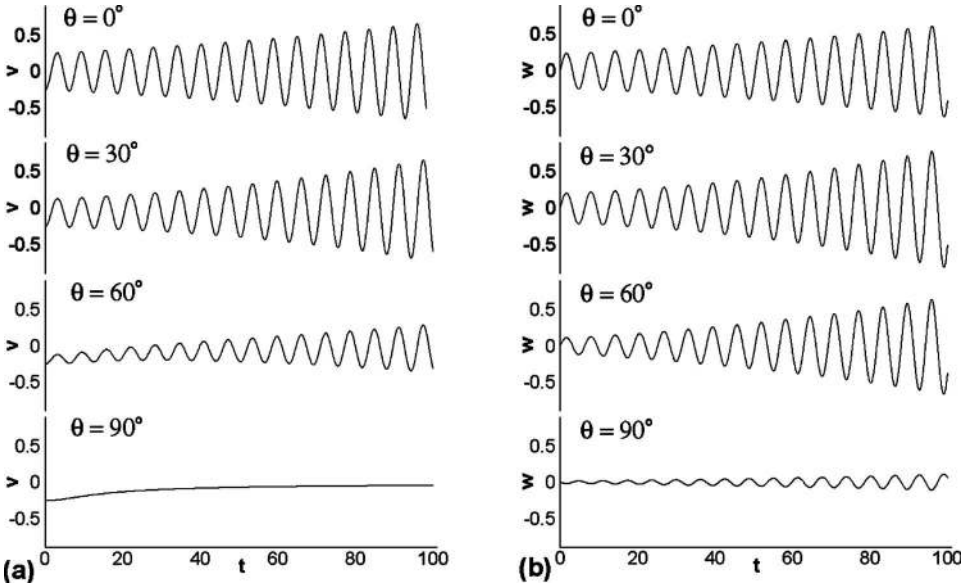

FIG. 5. Transverse velocity signal of a fluid particle for four different angular orientations of the skewed Rankine vortex pair (α=1.0, β=−1.0, ε=2.0; x_0=0.0, y_0=0.0, z_0=2.0; t=100): (a) y component of velocity and (b) z component of velocity.

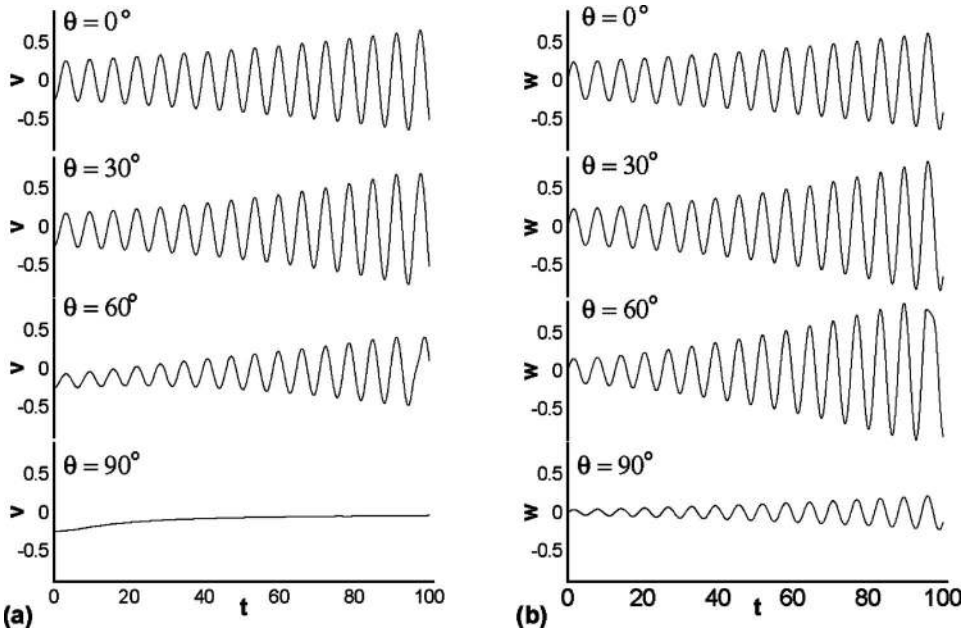

FIG. 7. Transverse velocity signal of a fluid particle for four different angular orientations of the skewed Rankine vortices ($\alpha=1.0$, $\beta=-1.0$, $\varepsilon=2.0$, $u_0=0.05$; $x_0=0.0$, $y_0=0.0$, $z_0=2.0$; $t=100$) with a superimposed uniform velocity in the x direction: (a) y component of velocity and (b) z component of velocity.

C. Effect of axial separation for a parallel system

Figures 8(a)–8(d) present paths of a fluid particle in the field of a parallel counter-rotating Rankine vortex pair for $\alpha=1$, $\beta=-1.0$. The axial half-separation of the skewed pair is varied from $\varepsilon=1.8$ to 2.6. For all the paths corresponding to different values of ε, the initial position of the fluid particle remains the same as before, viz., $x_0=0.0$, $y_0=0.0$, and $z_0=2.0$. It is observed from Figs. 8(a)–8(d) that the fluid particle for all values of ε follows an expanding helical path revolving around the nearer vortex. This is because an increase in ε results in a decrease in the influence of the other vortex on the particle, producing a larger velocity contribution from the first vortex. Figures 9(a) and 9(b) present transverse velocity signals, v and w, respectively, of the fluid particle corresponding to four different orientations of the vortex pair.

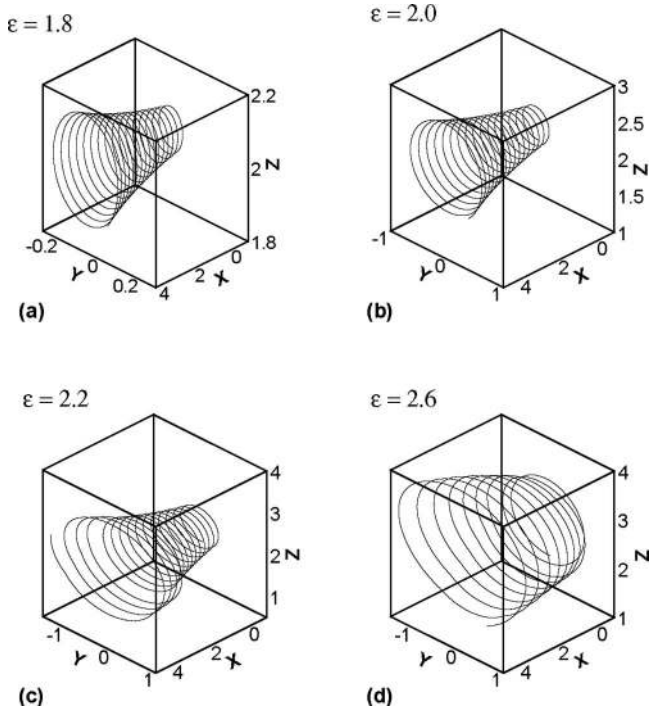

FIG. 8. Path of a fluid particle for parallel counter-rotating Rankine vortices with different axial distances ($x_0=0.0$, $y_0=0.0$, $z_0=2.0$; $t=100$) with a superimposed uniform velocity in the x direction ($u_0=0.05$).

D. Effect of wall confinement on the parallel system

Figures 10(a)–10(c) show the paths of a fluid particle in the field of a parallel, counter-rotating Rankine vortex pair confined by walls normal to the y axis. The axial half-separation is kept as $\varepsilon=2.0$ and the initial position of the fluid particle remains the same as in previous cases. The channel confinement is expressed as H/a, where H is the separation between the parallel walls and a is the core radius. For larger values of confinement, the path of the fluid particle remains expanding helical type [Fig. 10(a)] until $t=500$. However, with decrease in the confinement, the expansion of the helical path is restricted by the confining walls. Figures 10(b) and 10(c) clearly confirm the observation. Figures 11(a) and 11(b) present the temporal evolution of the y and z components of the velocity of the fluid particle, respectively, for three different values of wall confinement. It is apparent that for smaller values of confinement, the amplitude of both the transverse velocity components decreases.

E. Interaction of longitudinal vortices in the channel flow

Consider the flow situation where a uniform flow enters a rectangular channel confining a delta wing type of vortex generators mounted at the midplane of the channel. The kinematic equations governing the Lagrangian motion of a representative fluid particle which is initially located at the inlet of the channel ($x_0=0$) are obtained by superposition of the

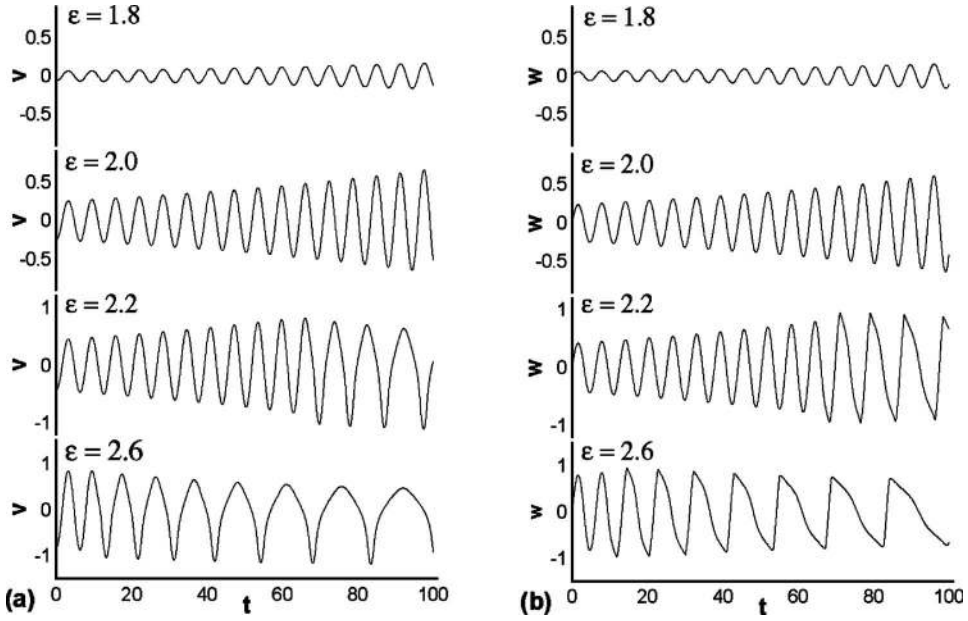

FIG. 9. Transverse velocity of a fluid particle for parallel counter-rotating Rankine vortices with different axial separations (x_0=0.0, y_0=0.0, z_0=2.0; t=100) with a superimposed uniform velocity in the x direction (u_0=0.05): (a) y component of velocity and (b) z component of velocity.

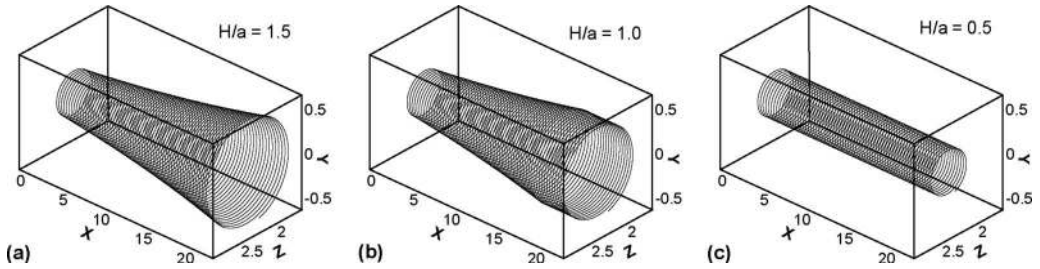

FIG. 10. Path of a fluid particle for parallel skewed counter-rotating Rankine vortices (x_0=0.0, y_0=0.0, z_0=2.0; t=500) with a superimposed uniform velocity in the x direction (u_0=0.05) for different confinements: (a) H/a=1.5, (b) H/a=1.0, and (c) H/a=0.5.

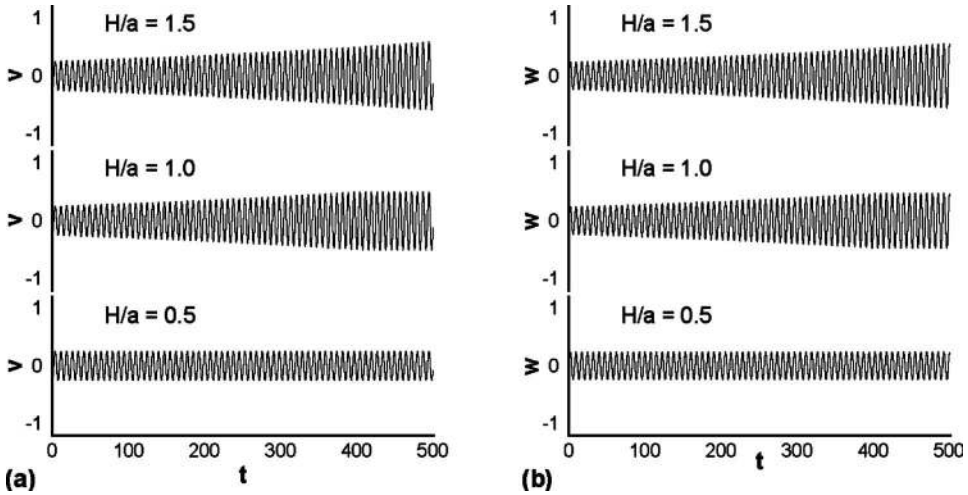

FIG. 11. Velocity of a fluid particle for parallel skewed counter-rotating Rankine vortices (x_0=0.0, y_0=0.0, z_0=2.0; t=500) with translational velocity in the x direction (u_0=0.05) with different confinements.

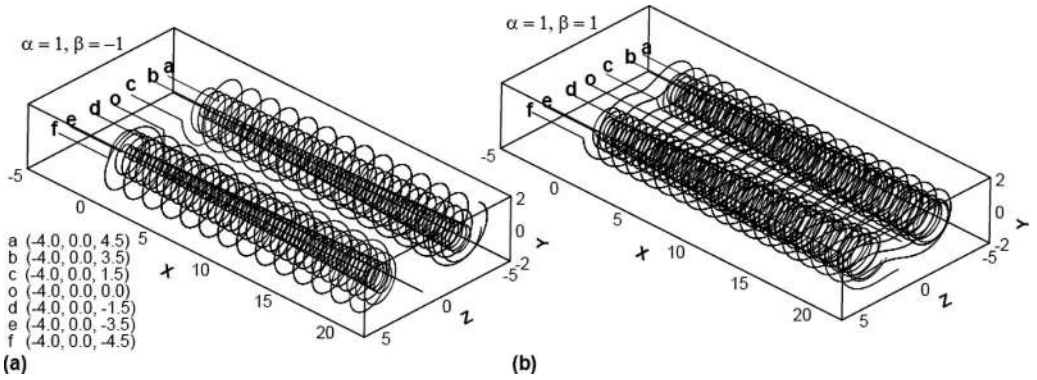

FIG. 12. Path of six different fluid particles entering a confined channel ($H/a=4.0$) in the x direction ($u_0=0.05$) in the field of parallel semi-infinite Rankine vortices with axial separation of $\varepsilon=3.0$: (a) counter-rotating and (b) corotating.

uniform flow and the semi-infinite vortex field derived from Eqs. (6a)–(6c). The resulting dynamical system for $x<x_1$ becomes

$$\frac{dx}{dt}=u_0,$$

$$\frac{dy}{dt}=0, \tag{9a}$$

$$\frac{dz}{dt}=0,$$

and for $x\geq x_1$, it becomes

$$\frac{dx}{dt}=u_0,$$

$$\frac{dy}{dt}=-\frac{\alpha(z+\varepsilon)}{A_1}-\frac{\beta(z-\varepsilon)}{A_2}, \tag{9b}$$

$$\frac{dz}{dt}=\alpha\frac{y}{A_1}+\frac{\beta y}{A_2},$$

where $x=x_1$ is the position from the inlet in the flow direction beyond which the field of longitudinal vortices sets in.

Figures 12(a) and 12(b) present the paths of different fluid particles in the field of parallel vortices due to vortex generators in counter-rotating and corotating configurations, respectively. The considered fluid particles are initially located at the inlet to the channel in its midplane (the plane of vortex system) at $x=-4$ and the vortex field exists beyond $x=0$, i.e., the position of the leading edge of vortex generators. Initially, the fluid particles enter the channel with an initial uniform velocity of $u_0=0.05$. The axial half-separation for the vortex pair is maintained as $\varepsilon=3.0$ and the channel height is $H/a=4.0$. It may be observed from Fig. 12(a) that for the counter-rotating configuration, the fluid particles (a–f) move along a helical path about the axis of the vortex that has a stronger influence on the fluid particle. The helical paths observed for particles a–f do not remain completely cylindrical due to the influence of the other vortex. Moreover, for the fluid particle initially located at position o, there occurs a continuous transverse shift during translation along the axis of the vortex pair. On the other hand, for the same initial motion of the fluid particles, the effect of the corotating vortex pair is interestingly different from that of the counter-rotating pair, as can be seen from Fig. 12(b). The fluid particle initially located at o follows a straight path along the x direction due to the effect of uniform flow, as expected. In Fig. 12(b), fluid particles b–e move in helical paths around the nearer vortex axis because of the stronger influence of the vortex that is closer to their starting point. However, the particles starting from positions a and f are seen to move in a helical path which envelopes both the vortices simultaneously. If the vortex pair is not fixed and if axial separation of the two vortices becomes of the order of the sum of their core radii, due to vortex diffusion, the core shape would become unsteady and phenomena such as vortex merging would take place, as discussed by Meunier *et al.*[7] Finally, for the system of the counter-rotating pair, it is found that the fluid particle motion remains constrained to revolve around the vortex with the stronger influence. Consequently, no possibility of core merging exists for the case of the counter-rotating vortex pair. On the other hand, for the system of corotating vortices shown in Fig. 12(b), core deformation or merging may take place if the vortex filaments are not fixed. Paulo *et al.*[17] investigated the Reynolds number dependence of two-dimensional laminar corotating vortex merging. Josserand and Rossi[18] also studied numerically the rapid phases of merging of a corotating vortex pair.

V. CONCLUSIONS

The general velocity field equations have been derived for a skewed Rankine vortex pair with inclined axes. The dynamical system governing the kinematics of a Lagrangian particle has been obtained by a simple superposition of the velocity fields of the two vortices. The proposed dynamical system has been solved to examine the existence of fixed points. It is found that for the skewed vortex pair with oblique axes, no real fixed points exist. However, there exist *three* real fixed points for the parallel and corotating configuration and *two* real fixed points for the parallel and counter-rotating configuration of the vortex pair. The analytical formulation is expected to be useful in carrying out investigations to study the mechanism by which particle ad-

vection contributes toward enhancement in flow mixing and heat transfer in interacting vortex fields. The formulation has been used to study the path of a uniformly translating fluid particle under the influence of a semi-infinite vortex field in counter-rotating and corotating configurations. The vortex field confined by wall surfaces mimics the situation of longitudinal vortices generated by vortex generators mounted on fins of heat exchangers.

[1] M. Jacobi and R. K. Shah, "Heat transfer surface enhancement through the use of longitudinal vortices: A review of recent progress," Exp. Therm. Fluid Sci. **11**, 295 (1995).
[2] R. Romero-Mendez, M. Sen, K. Yang, and R. McLain, "Enhancement of heat transfer in an inviscid-flow thermal boundary layer due to a Rankine vortex," Int. J. Heat Mass Transfer **41**, 3829 (1998).
[3] H. Moffatt, "The interaction of skewed vortex pairs: A model for blow-up of the Navier–Stokes equations," J. Fluid Mech. **409**, 51 (2000).
[4] C. M. Casciola and R. Piva, "A Lagrangian approach for vorticity intensification in swirling rings," Comput. Mech. **21**, 276 (1998).
[5] D. W. Moore and P. G. Saffman, "The motion of a vortex filament with axial flow," Philos. Trans. R. Soc. London, Ser. A **272**, 403 (1972).
[6] P. G. Saffman, *Vortex Dynamics* (Cambridge University Press, Cambridge, England, 1992).
[7] P. Meunier, U. Ehrenstein, T. Leweke, and M. Rossi, "A merging criterion for two-dimensional co-rotating vortices," Phys. Fluids **14**, 2757 (2002).
[8] S. Le Dizes and A. Verga, "Viscous interactions of two co-rotating vortices before merging," J. Fluid Mech. **467**, 389 (2002).
[9] E. D. Siggia, "Collapse and amplification of a vortex filament," Phys. Fluids **28**, 794 (1985).
[10] J. M. Ottino, *The Kinematics of Mixing: Stretching, Chaos and Transport* (Cambridge University Press, Cambridge, England, 1989).
[11] G. K. Batchelor, *An Introduction to Fluid Mechanics* (Cambridge University Press, Cambridge, England, 1967).
[12] H. Aref and N. Pomphrey, "Integrable and chaotic motion of four vortices. I. The case of identical vortices," Philos. Trans. R. Soc. London, Ser. A **380**, 359 (1982).
[13] R. Vasudevan, V. Eswaran, and G. Biswas, "Winglet-type vortex generators for plate-fin heat exchangers using triangular fins," Numer. Heat Transfer, Part A **38**, 533 (2000).
[14] S. Tiwari, P. L. N. Prasad, and G. Biswas, "A numerical study of heat transfer in fin-tube heat exchangers using winglet-type vortex generators in common-flow down configurations," Prog. Comput. Fluid Dyn. **3**, 32 (2003).
[15] H. Aref, "Stirring by chaotic advection," J. Fluid Mech. **143**, 1 (1984).
[16] D. W. Jordan and P. Smith, *Nonlinear Ordinary Differential Equations*, 2nd ed. (Clarendon, Oxford, 1987).
[17] J. S. A. Paulo, F. de Sousa, and J. C. F. Pereira, "Reynolds number dependence of two-dimensional laminar co-rotating vortex merging," Theor. Comput. Fluid Dyn. **19**, 65 (2005).
[18] Ch. Josserand and M. Rossi, "The merging of two co-rotating vortices: A numerical study," Eur. J. Mech. B/Fluids **26**, 779 (2007).